# Voltage Profile Analysis in Distribution Network for Allowable Hosting Capacity from PV Integration

Anju Yadav
Department of Electrical Engineering
MNNIT
Allahabad, India
anjupyadav1994@gmail.com

Nand Kishor
Department of Engineering
Østfold University College
Fredrikstad, Norway
nand.kishor@hiof.no

Richa Negi
Department of Electrical Engineering
MNNIT
Allahabad, India
richa@mnnit.ac.in

2022 1st International Conference on Sustainable Technology for Power and Energy Systems (STPES) | 978-1-6654-5915-0/22/$31.00 ©2022 IEEE | DOI: 10.1109/STPES54845.2022.10006593

***Abstract*—A high amount of PV integration into the low voltage distribution network is a major issue; it may cause contrary grid effects in terms of voltage unbalance and system instability. Thus, the best location for PVs placement and their maximum capacity needs to be determined. In this study, a novel approach based on the calculation of the local impedance index is considered. This calculation is carried out for different areas in the network and for PV integration upto 100% to decide both the most suited area and maximum allowable hosting capacity (HC). The simulation uses GridPV and OpenDSS toolbox/platform for performing the study. It is shown that with the approach applied, it is possible to keep the voltage violations limited, mainly at far-end feeder buses.**

***Keywords—Photovoltaic (PV), Voltage violation, Voltage stability, Local Impedance Index, Hosting capacity***

## I. INTRODUCTION

Many researchers promote small scale renewable integration because of fuel cost and postponement of infrastructure improvement [1-2], but unsuited arrangement of photovoltaic (PV) sources in terms of site location and inverter size [3-4] may cause negative impact on total cost, power loss, and voltage violation. The PV integration level, system parameters, and load profile are some important factors that impact the cost positively or negatively [5-6]. Studies [7-9] specify that high PV penetration level can help to reduce losses but high PV integration also induce reinforcement required for system, accounts for voltage instability and losses.

The studies on distributed generations (DGs) location and size has been extensively reported in recent years. These fall in the category of planning and operational, distribution network and DG models, inclusion of uncertainty in renewable generation/load and optimal solution approach. Among several analytical techniques for the optimal planning of renewable integration follows mathematical formulation of network, with set of numerical equations, defining in the form of an objective function. The review discussion on the subject [10] enlists several optimization techniques formulated on multi-objective functions to determine the optimal size of PVs. It is agreed that integration level depends on several factors, including load profile, power-generation match, etc, but in these literatures, PV integration as high as 45% has been discussed. In [11], results indicate that optimal power factor can reduce loss and improve voltage stability as compared to PV operation at unity power factor. But, complex analytical techniques, involving objective functions, require computation of Jacobian matrix, resulting in increased computational burden.

PV inverters operated at a fixed power factor can provide reactive power into the network to compensate against voltage rise due to reverse power flow at the time of high power generation. However due to lack of robust communication information exchange, the power factor of PV inverters cannot be changed, whenever, there is an increase in power from PV system or a change in weather conditions [14]. As such, PV inverters are expected to operate with multiple functionalities.

The low voltage distribution network is usually unbalanced and have both single- and three-phase loads connected. Due to unevenly distributed single-phase loads and asymmetrical line impedances, the prevailing voltage unbalance may lead to increased network losses and even instability in the system [15-16]. The integration of a high amount of PVs will further aggravate the unbalance level due to changes in the loading pattern of the network, thereby influencing the performance of voltage regulation capability of inverters. The participation of PV inverters in voltage control depends on their reactive power capability and active power modulation. Accordingly, the behavior of unbalance network in response to the location of PV and its size will be governed not only by the operating conditions (disturbances) but also by the network characteristic. For example, the high R/X ratio in the network causes voltage magnitude to be more sensitive to active power injection as compared to reactive power. A well-known issue also discussed later in the manuscript is the voltage violations, particularly at far-end feeders, even with low (2%, 5%) PV integration. Additionally, the transient solar radiation profile can lead to increased voltage variability across the network.

In [17] a distributed control strategy using the dynamic formation of coalitions is introduced to adjust more PV inverters to regulate voltage. A comparison between Fixed power factor (FPF) and Volt-VAR is executed [18] according to voltage regulation capabilities. In [19] comparison between different control schemes is discussed to reduce over-voltage (OV) violation on high PV integration with results simulated using OpenDSS platform. The effect of solar uncertainty and location of a centralized solar plant using wavelet variability model (WVM) is modelled in [20] and a case study is performed to review the reactive power capability for existing control schemes towards voltage regulation in [21].

The placement can be planned on upstream buses of the feeder to successfully reduce the voltage deviation with high PV integration [12]. The hosting capacity (HC) of PV is alterable based on the location of PV DGs and implemented control strategies towards voltage violations [13], thus

978-1-6654-5915-0/22/$31.00 ©2022 IEEE

maximum HC is important to be determined so that no voltage violation occurs.

In the present study, analysis is performed to determine the most suitable area of the distribution network for PV placement in distributed form. In other words, the best area of the distribution network is determined for PV placement and its amount so that there are no voltage violations, mainly at feeder-end buses. The planning of PV placement is based on the calculation of local impedance index (LII), calculated over a range of PV integration in the network and subsequently analyzing the voltage violations to decide on the allowable HC.

This paper is organized as; Section II describes modelling of the network and use of the simulation platform, followed by an analytical calculation of LII and selection of area for PV placement. Next, section IV presents the results on bus power, line loss, and voltage analysis for chosen HC with different solar radiation profiles and finally, Section 5 concludes the work.

## II. Distribution Network Modelling And Simulation Platform

In the study, the open-source distribution system software (OpenDSS), developed by the Electric Power Research Institute, and GridPV toolbox, developed by SANDIA National Laboratories are used. In OpenDSS, a 3-phase distribution network load flow analysis can be solved, including unbalanced phases, DGs integration, and future smart grid applications [22]. The GridPV toolbox [23] is run in the MATLAB platform. Using these tools, the distribution network and solar PV system can be easily modelled. They also support the simulation of a high-resolution time-series power flow analysis, particularly against solar radiation. The complete modelling and analysis with the integration of OpenDSS and MATLAB (GridPV) is provided through a COM server interface.

The IEEE-37 bus distribution network is divided into four areas; Area 1- Area 4, with specified bus number as represented in Fig. 1(a), to analyse the placement of PV and integration amount on voltage profile. Further, as indicated in said figure, these areas are demarcated into Region 1 and Region 2. The solar radiation profile characterized by both amount and its magnitude variation are considered as shown in Fig. 1(b). As can be seen, the first half portion is identified as the largest magnitude variation, while the remaining half has a large amount of radiation, but with the least magnitude variation. The solar radiation is sampled at a rate of 2s.

Fig. 2 illustrates the interface of two toolboxes. In the GridPV toolbox, Wavelet Variability Model (WVM) [23] is applied to convert solar radiation data, smoothening the variability to compute PV system size and the density in the given area. The circuit buses of the distribution network are placed in latitude and longitude coordinates, with density of the PV system representing the amount of land area. In the study, distributed PV is placed according to specified areas (Fig. 1(a)) for different integration amounts (MW size) in the percentage of total load in the distribution network. Next, the power factor is defined, representing the absorption/injection of VARs via PV smart inverter. With chosen area for PV placement and its size (MW), information is stored in a .mat file to be added to the OpenDSS platform, which creates a .dss file. The given PV system data and solar radiation data are created in both the .txt file and .dss file for objects in OpenDSS. The GridPV toolbox initializes the COM interface in MATLAB to communicate with the OpenDSS in loading and compiling distribution network (circuits) for analysis. Now, time-series analysis is performed in OpenDSS to understand the impact of the variability of solar radiation and PV placement on voltage profile. For every placement of PV capacity (integration) in each area, as discussed in the next section, the LII value is calculated for voltage violation analysis.

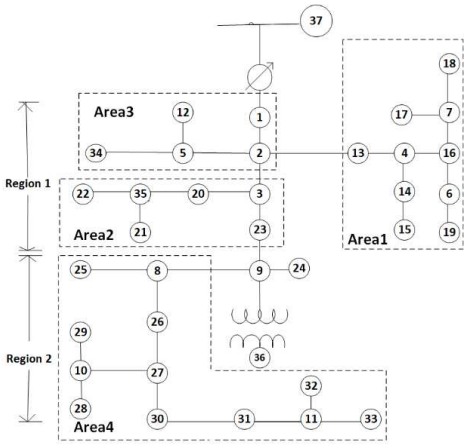


(a) IEEE-37 bus distribution network

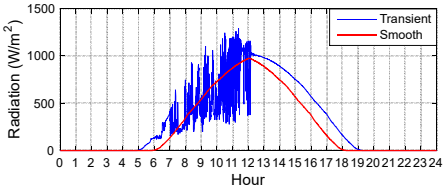


(b) Typical solar radiation profile

Fig. 1. Distribution network and solar radiation profile.

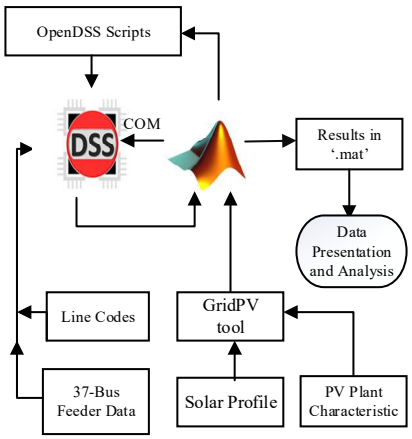


Fig. 2. Flowchart of the MATLAB-OpenDSS interfacing.

## III. Analytical Calculation For PV Placement Area

With the GridPV toolbox, having the distribution network represented in the form of bus coordinates, it is possible to visualize the network power lines. This enables modelling of the PV system based on its location, capturing the location-dependent value. The PV integration level, $P_{PV}^{A_j}$ in a given area $A_j$, is defined as the ratio of the total

DC power rating of the PV system (inverter) installed to the total load demand in the distribution network, given as:

$$P_{PV}^{A_j} = \frac{\sum_{k=1}^{N_k} P_{PV,k}}{\sum_{l=1}^{N_l} P_l} \quad (1)$$

where, $N_k$ is the total number of buses with PV installed in a given area, $N_l$ is the total number of load buses in the distribution network. The PVs are installed at the load bus in a given area. The deployment of PV system in a given area is considered based on the calculated value of local impedance index (LII).

### *A. Analysis for Suitable Areas*

The LII is calculated at each bus in different areas after placement of PV system in distributed form. Consider the local impedance at every load bus to be defined as

$$Z_{N_k} = \frac{V_{N_k}^{(1)}}{I_{N_k}^{(1)}} \quad (2)$$

where, $V_{N_k}^{(1)}$ and $I_{N_k}^{(1)}$ is voltage and current respectively at every load bus for base load condition, i.e. without PV integration. Consider $V_{N_k}^{(2)}$ and $I_{N_k}^{(2)}$ as voltage and current respectively after PV placement of a certain percentage in the given area. Then, LII is defined as:

$$Z_{N_k}^{LII} = \frac{V_{N_k}^{(2)} - V_{N_k}^{(1)}}{I_{N_k}^{(2)} - I_{N_k}^{(1)}} \quad (3)$$

The average value of LII, $Z_{av}^{LII}$ in a given area is calculated from

$$Z_{av}^{LII} = \frac{Z_{N_k}^{LII}}{N_k} \quad (4)$$

The complete steps adopted in the calculation of LII for each area at every PV integration level in the distribution network is illustrated in the flow chart shown in Fig. 3. The complete distribution network is divided into areas A1–A4 according to the geographical location from the main (grid) substation. Equation (2) for base condition, i.e., without PV integration LII is computed. With the integration of a 2% PV system in A1, LII is determined as per (3)-(4) for all the three phases and buses in the network. The voltage at every bus in the network is checked if there are no voltage violations. Similarly, the amount of PV integration in A1 is increased by 5%, 10%, 15%, 20%, 50%, 80% & 100%, and subsequently average LII is computed and voltage profile is checked. Next, PV integration is applied in the A2 area and the above steps are repeated. Following the above stated steps, the area that has the least value of LII and minimum voltage violations is considered most suitable location for integration of PV system. The minimum PV capacity associated without any voltage violation is the hosting capacity (HC) of that area.

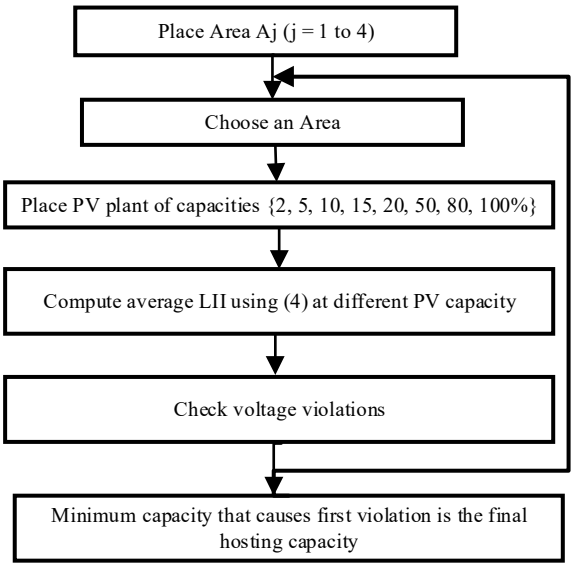


Fig. 3. Flowchart of the load flow based LII approach.

Fig. 4 represents the average LII of each area for PV placement in A1-A4. The value of average LII is compared for PV placement in different areas. As indicated, the lowest LII values are achieved for PV placement in A1 and A3. It may be said that the distribution network will remain without voltage violations if PV is placed in these two areas as compared to A2 and A4. Thus, A1 and A3 is the most-suited location for PV placement and needs further investigation in respect to voltage variations in these areas.

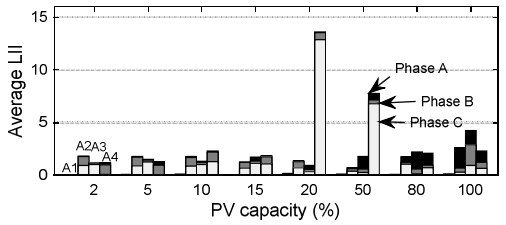


(a) For PV placement in A1

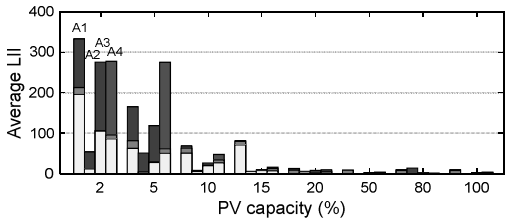


(b) For PV placement in A2

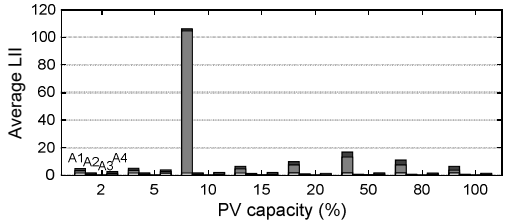


(c) For PV placement in A3

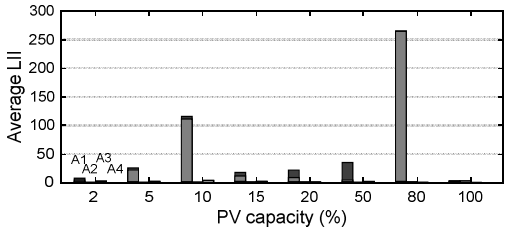

(d) For PV placement in A4

Fig. 4. Average LII for PV placement in different areas.

### B. *Voltage Analysis for Suitable Areas*

In the process to determine the best location for PV placement in the distribution network, next, a voltage profile analysis is performed for A1 and A3. The phase voltage distribution at the buses for PV integration upto 100% capacity is shown in Fig. 5. In the plot, on x-axis, the bus position as a distance from substation is indicated. The undervoltage (UV) can be observed on load buses of Region 2 in phase A at 2% PV (bus-10, 28, 29, 11, 33, 32, 27, 30, 21), and 5% PV capacity (bus-11, 33, 32, 30, 31). The overvoltage (OV) is depicted at most of the buses in phase A and phase C, with the integration of PV capacity in the range of 50-100%. Also, for PV capacity greater than 80%, some buses corresponding to phase B violate.

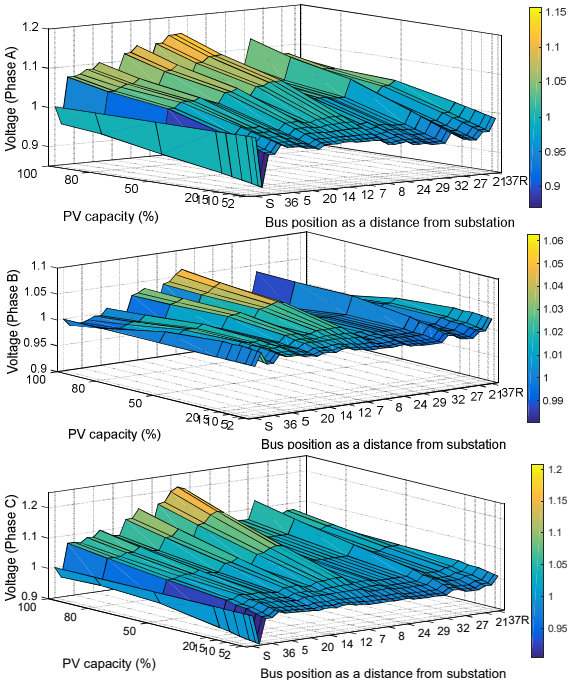


Fig. 5. Voltage profile for PV placement in A1.

When PV is placed in A3, the UV can be observed in phase A at bus-10, 28, 29, 11, 33, 32, 27, 30, 21, and bus-28, 11, 33, 32, 30, 31 for PV integration of 2% and 5% respectively as represented in Fig. 6. When PV capacity is between 80-100%, then OV is observed in phase B at bus-34. On comparing, the results for PV placement in A1 and A3, voltage profile of A3 remains more stable as PV capacity is increased. Thus, A3 is most suited for PV placement as compared to A1. The voltage violations get more prominent with integration of PV capacity more than 50%. So HC in this case is 50%.

The real power of total numbers of inverter (size) for PV system placed in A1 and A3 is shown in Fig. 7. The said figure indicates the total capacity installed in a phase and its corresponding bus for increase in PV integration level. The load connected in IEEE-37 bus system at base load condition is 538 kW, 252 kW, 808 kW, and 774 kW in A1, A2, A3 and A4 respectively. With 50% PV integration, the total capacity (kW) of inverter is 3435.5 kW and 3224.4 kW in A1 and A3 respectively. For increased PV integration above 50%, the total capacity of installed PV (inverter) is higher in A1 as compared to A3.

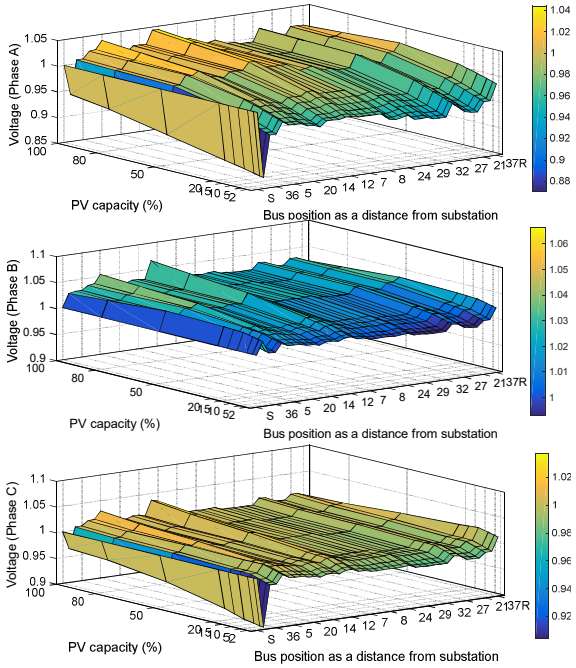


Fig. 6. Voltage profile for PV placement in A3.

## IV. Result And Discussion

With the above discussion, it is clear that PV installation with hosting capacity of 50% can be considered in A3, so that there are no serious voltage violations. But further investigation is discussed before making a firm conclusion out of this study. In this section, firstly, analysis is performed on available power at the bus and the line loss. Next, the voltage profile at far-end bus in the network is obtained.

### A. *Bus Power and Line Loss*

The power installed at each phase of load buses available in A3 for pf=1 and pf=0.9 is represented in Fig.8. There is no difference in power for transient and smooth radiation. So, results for PV placement in A3 with 50% PV capacity for transient radiation is represented below. The

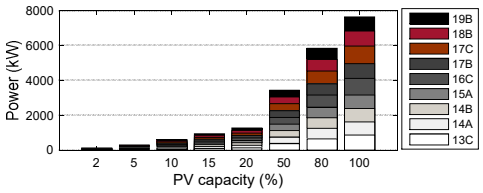

(a) A1

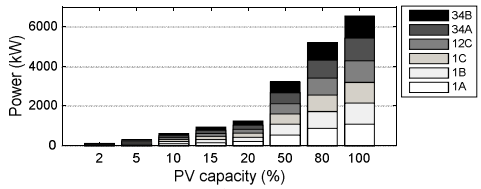


(b) A3

Fig. 7. Size (kW) of PV inverter.

power loss in each line is represented in Fig. 9. At power factor (pf) =1 (unity), total loss is 69.6 kW (line loss= 47.4 kW, transformer loss=22.1 kW), while total load power is 2461.3 kW. So, total power loss for the circuit is 2.83%. At pf=0.9, total loss is 49.9 kW (line loss= 43.9 kW, transformer loss=5.9 kW), accounting for total circuit loss of 2.02%. Further, the hosting capacity is carried out for smooth variation of solar radiation (Fig.1(b)). In this type of variation, the total power loss with PV placement in A1, A2, A3 and A4 accounts for 5.35%, 5.83%, 2.83% and 6.10% respectively. Thus, among these four areas, the power loss is least, when PV system is placed in A3.

### *B. Analysis of voltage profiles at 50% capacity (HC) for different solar radiation*

The voltage profile obtained at unity power factor for transient solar radiation is illustrated in Fig. 10(a). In this case, the voltage is increases with increase in radiation and the transients in voltage profile at feeder-end buses is observed before 12:00 pm and then voltage is slightly reducing until 5:30 pm. Thereafter, the voltage profile becomes stable and remains constant. On other hand, with pf=0.9 as shown in Fig. 10(b), here, voltage overshoots is not observed in any phase, while oscillations are indicated in all the three phases between 7:00-11:30 am.

The results are also verified for smooth solar radiation profile at pf=0.9, associated with least magnitude variations as shown in Fig. 11.

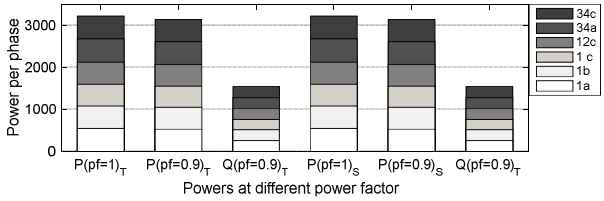


Fig. 8. Active and reactive power on each bus for transient radiation placement in A3

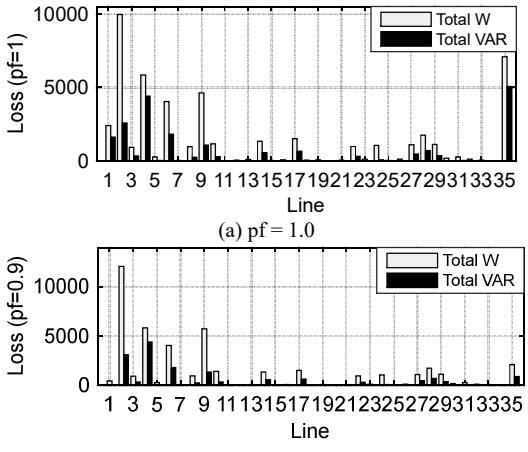


(a) pf = 1.0

(b) pf = 0.9

Fig. 9. Line loss in the network

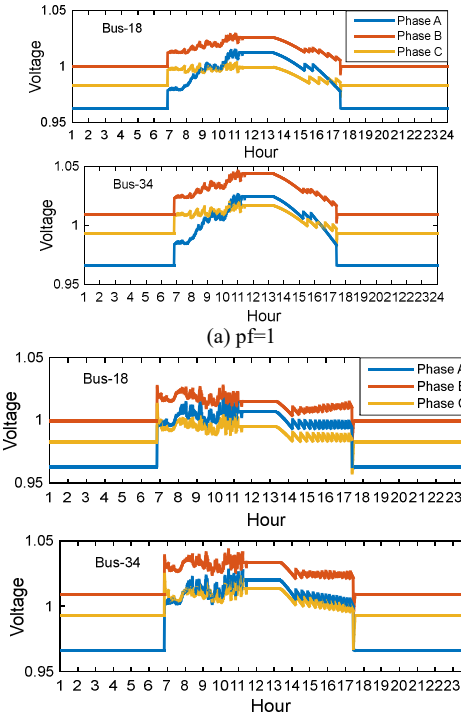


(a) pf=1




(b) pf=0.9

Fig. 10. Voltage profile of feeder-end bus under transient solar radiation profile

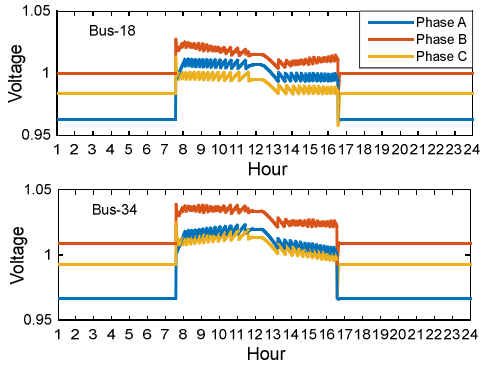


Fig. 11. Voltage profile of feeder-end buses at pf=0.9 for smooth solar radiation

## V. CONCLUSION

In this work, a LII based approach was used to determine area for PV placement and its integration amount to limit the voltage violations. In the study, hosting capacity of PV system was fixed that meets the criteria of voltage violations. The analysis was performed mainly to investigate the variation of voltage at far-end feeder buses. This study was performed in GridPV and OpenDSS platforms on the IEEE-37 bus network, with a load-flow based approach in OpenDSS.

It was shown that voltage variation remained stable, particularly at far-end feeder buses for hosting capacity upto 50%.

## REFERENCES

[1] A. Keane, L. F. Ochoa, C. L. Borges, G. W. Ault, A. D. Alarcon-Rodriguez, R. A. Currie, F. Pilo, C. Dent, and G. P. Harrison, "State-of-the-art techniques and challenges ahead for distributed generation planning and optimization," IEEE Transactions on Power Systems, vol. 28, no. 2, pp. 1493–1502, May 2013.

[2] P. S. Georgilakis and N. D. Hatziargyriou, "Optimal distributed generation placement in power distribution networks: Models, methods, and future research," IEEE Transactions on Power Systems, vol. 28, no. 3, pp. 3420–3428, Aug 2013.

[3] A. J. Valdberg and M.W. Dwyer, "Distribution resources plan rulemaking (R. 14-08-013) locational net benefit analysis working group final report," Mar. 2017. [Online]. Available: http://drpwg.org/wpcontent/uploads/2016/07/R1408013-et-al-SCE-LNBA-Working-Group Final-Report.pdf

[4] M. M. Kamal, I. Ashraf, and E. Fernandez, "Optimal planning of renewable integrated rural microgrid for sustainable energy supply," Energy Storage, e332, https://doi.org/10.1002/est2.332

[5] A. Picciariello, K. Alvehag, and L. Soder, "Impact of network regulation on the incentive for DG integration for the dso: Opportunities for a transition toward a smart grid," IEEE Transactions on Smart Grid, vol. 6, no. 4, pp. 1730-1739, Mar 2015.

[6] S. A. Janko, M. R. Arnold, and N. G. Johnson, "Implications of high-penetration renewables for ratepayers and utilities in the residential solar photovoltaic (PV) market," Applied Energy, vol. 180, pp. 37-51, Oct 2016.

[7] M. A. Cohen and D. S. Callaway, "Effects of distributed PV generation on california's distribution system, part 1: Engineering simulations," Solar Energy, vol. 128, pp. 126–138, Apr 2016.

[8] S. M. Agah and H. A. Abyaneh, "Quantification of the distribution transformer life extension value of distributed generation," IEEE Transactions on Power Delivery, vol. 26, no. 3, pp. 1820–1828, Jan 2011.

[9] S. M. Agah and H. A. Abyaneh, "Distribution transformer loss-of-life reduction by increasing penetration of distributed generation," IEEE Transactions on Power Delivery, vol. 26, no. 2, pp. 1128–1136, Jul 2011.

[10] A. Ehsan and Q. Yang, "Optimal integration and planning of renewable distributed generation in the power distribution networks: A review of analytical techniques," Applied Energy, vol. 210, pp. 44-59, 2018.

[11] D. Q. Hung, N. Mithulananthan, and R. C. Bansal, "Integration of PV and BES units in commercial distribution systems considering energy loss and voltage stability," Applied Energy, vol. 113, pp. 162–70, Jan 2014.

[12] C. Luo, H. Wu, Y. Zhou, Y. Qiao, and M. Cai, "Network partition-based hierarchical decentralised voltage control for distribution networks with distributed PV systems," International Journal of Electrical Power and Energy Systems, vol. 130, pp.106929, Sep 2021.

[13] A. Ali, K. Mahmoud, and M. Lehtonen, "Maximizing hosting capacity of uncertain photovoltaics by coordinated management of OLTC, VAR sources and stochastic EVs," International Journal of Electrical Power and Energy Systems, vol. 127, pp. 106627, May 2021.

[14] Y. Takasawa, S. Akagi, S. Yoshizawa, H. Ishii, and Y. Hayashi, "Effectiveness of updating the parameters of the Volt-VAR control depending on the PV penetration rate and weather conditions," In2017 IEEE Innovative Smart Grid Technologies-Asia (ISGT-Asia), Auckland, NZ, December 4-7, 2017, IEEE, 2017. pp. 1-5. 10.1109/ISGT-Asia.2017.8378328.

[15] Y. Wang, N. Zhang, H. Li, J. Yang, and C. Kang, "Linear three-phase power flow for unbalanced active distribution networks with PV nodes," CSEE Journal of Power Energy System, vol. 3, no. 3, pp. 321-324, Sep 2017.

[16] Y. Liu, J. Li, and L. Wu, "Coordinated optimal network reconfiguration and voltage regulator/der control for unbalanced distribution systems," IEEE Transactions on Smart Grid, vol. 10, no. 3, pp. 2912-2922, May 2019.

[17] Y. Long, R. T. Elliott, and D. S. Kirschen, "Adaptive coalition formation-based coordinated voltage regulation in distribution networks," IEEE Transactions on Power Systems, pp. 1-1, Oct 2021, doi: 10.1109/TPWRS.2021.3120195.

[18] K. Rahimi, A. Tbaileh, R. Broadwater, J. Woyak, and M. Dilek, "Voltage regulation performance of smart inverters: Power factor versus Volt-VAR control," North America Power Symposium (NAPS), Morgantown, WV, USA, September 17-19, 2017, IEEE, 2017. pp. 1-6. 10.1109/NAPS.2017.8107407.

[19] J. Seuss, M. J. Reno, M. Lave, R. J. Broderick, and S. Grijalva, "Advanced inverter controls to dispatch distributed PV systems," IEEE 43rd Photovoltaic Specialists Conference (PVSC), Portland, OR, USA June 5-10, 2016, IEEE, 2016. pp. 1387-1392. 10.1109/PVSC.2016.7749842.

[20] M. Emmanuel, R. Rayudu, and I. Welch, "Modelling impacts of utility-scale photovoltaic systems variability using the wavelet variability model for smart grid operations," Sustainable Energy Technologies and Assessments, vol. 31, pp. 292-305, Feb 2019.

[21] T. A. Nguyen, R. Rigo-Mariani, M. A. Ortega-Vazquez, and D. S. Kirschen, "Voltage regulation in distribution grid using PV smart inverters," In 2018 IEEE Power and Energy Society General Meeting (PESGM), Portland, OR, USA, August 5-10, 2018, IEEE, 2018. pp. 1-5.

[22] Electric power Research Institute (EPRI), opendsswiki; 2018b .https://sourceforge.net/p/electricdss/code/HEAD/tree/trunk/Distrib/EPRITestCircuits/.

[23] M. Reno, K. Coogan, Grid Integrated Distributed PV (GridPV). Technical Report, 2013.